LPV Model Development and Control of A Solution Copolymerization Reactor ☆

Sandy Rahme[a], Hossam S. Abbas[b], Nader Meskin[a,*], Roland Tóth[c], Javad Mohammadpour[d]

[a] *Department of Electrical Engineering, Qatar University, Doha, Qatar,* sandy.rahme, nader.meskin@qu.edu.qa

[b] *Electrical Engineering Dept., Faculty of Engineering, Assiut University, 71515 Assiut, Egypt,* hossam.abbas@aun.edu.eg

[c] *Control Systems Group, Eindhoven University of Technology, P.O. Box 513, 5600 MB Eindhoven, The Netherlands,* r.toth@tue.nl

[d] *Complex Systems Control Lab, College of Engineering, The University of Georgia, Athens, GA 30602, USA,* javadm@uga.edu

Abstract

In this paper, *linear parameter-varying* (LPV) control is considered for a solution copolymerization reactor, which takes into account the time-varying nature of the parameters of the process. The nonlinear model of the process is first converted to an exact LPV model representation in the state-space form that has a large number of scheduling variables and hence is not appropriate for control design purposes due to the complexity of the LPV control synthesis problem. To reduce such complexity, two approaches are proposed in this paper. First, an approximate LPV representation with only one scheduling variable is obtained by means of a *parameter set mapping* (PSM). The second approach is based on reformulating the nonlinear model so that it provides an LPV model with a fewer number of scheduling parameters but preserves the same input-output behavior. Moreover, in the implementation of the LPV controllers synthesized with the derived models, the unmeasurable scheduling variables are estimated by an extended Kalman filter. Simulation results using the nonlinear model of the copolymerization reactor are provided in order to illustrate the performance of the proposed controllers in reducing the convergence time and the control effort.

Keywords: Copolymerization reactor; Linear parameter-varying systems; Parameter set mapping; LPV control; Extended Kalman filter.

☆This publication was made possible by NPRP grant No. 5-574-2-233 from the Qatar National Research Fund (a member of Qatar Foundation). The statements made herein are solely the responsibility of the authors.

*Corresponding author. Phone:+974 4403 4224, Fax:+974 4403 4201,
Email address: nader.meskin@qu.edu.qa (Nader Meskin)

1. Introduction

Controlling the operation of polymer reactors is a highly important task that aims at maximizing the production rate and the product quality and also minimizing the transition losses due to the high consumer demands, as well as the tight market competition for producing different grades of polymers [1]. However, the control design task is nontrivial due to the nonlinear behavior of polymer reactor systems which exhibit strong dependence on multiple operating regimes [2], [3], [4]. Furthermore, polymer reactors exhibit unstable modes at some operating points [5], as well as time-varying parameters that need to be measured since a polymerization reactor switches through different operating points depending on the needed polymer grades [4]. Due to the existence of unmeasured disturbances influencing these systems, the development of a robust control strategy is highly desired. Several control approaches have been investigated in the literature [3], [4]. For example, a classical PID controller is developed in [6] without the need of an accurate dynamical model. However, PID controllers are not adequate to cope with such complex systems, in which strong interactions exist between the controlled variables. Hence, model predictive control (MPC) based on simple process models has been proposed in [3] and [7], where a rapid transition between two typical operating points is ensured. A nonlinear controller has been designed and validated experimentally in [2], which depends on online measurements of time-varying model parameters of a nonlinear model of the process.

Generally speaking, optimal control techniques are preferred if a good process model is available [1]. Moreover, adaptive control strategies can be applied in order to take the time-varying nature of the process into account, provided that online measurements/estimations are available. In this paper, linear parameter-varying (LPV) control techniques (see [8]) are considered to control a free radical solution copolymerization reactor described in [6]. LPV systems describe a class of nonlinear/time-varying systems that can be represented in terms of parametrized linear dynamics in which the model coefficients depend on a number of measurable variables called *scheduling variables* [9], [10](Ch.3). The LPV methods provide powerful tools for designing controllers for nonlinear/time-varying plants [11]. The LPV controller synthesis tools extend the well-known methods of controlling linear time-invariant (LTI) systems to control nonlinear systems with guaranteed stability and high performance over a wide range of operation [12], [13], [14].

The design of LPV controllers often involves two major problems: the presence of several scheduling variables in the LPV model, as is the case in the copolymerization reactor, and the conservatism arising from the overbounding of the range of variation of the scheduling variables [15]. For the standard LPV-$\mathcal{H}_\infty$ design approach with polytopic models [8], the number of linear matrix inequalities (LMIs) to be solved increases exponentially with the number of scheduling variables so the control synthesis problem becomes computationally

intractable [16]. On the other hand, overbounding the range of the scheduling variables often renders the LPV model to include some behaviors that are not exhibited by the original plant due to the dependence of the scheduling variables on the physical variables, which results in conservatism.

In this paper, an LPV representation of the copolymerization reactor is obtained through a transformation capturing the system nonlinearities in the scheduling variables. However, due to the existence of different nonlinear terms in the copolymerization reactor model, the obtained LPV model turns out to have 15 scheduling variables. Two approaches are then introduced for coping with the high number of scheduling variables. In the first approach, the number of scheduling variables is reduced via the *parameter set mapping* (PSM) procedure based on *principal component analysis* (PCA) [15]. The parameter set mapping is an effective way to reduce the conservatism in LPV modeling by *resizing* the scheduling range such that the reduced model matches the original system behavior as closely as possible [17], [18]. The second method is a specific model reduction approach aiming at reducing the complexity, as well as the number of scheduling variables of the model while the input-output behavior of the original system is preserved. This method is based on an alternative conversion of the nonlinear model to an LPV form by truncating the state variables that have no significant role in the state evolution.

Once the operating region and the resulting LPV models are determined, a control design methodology is applied on each produced model. For the LPV-PSM approach, LPV $\mathcal{H}_\infty$ control synthesis, introduced in [8], is used to synthesize a controller for the reduced LPV model of the reactor. For the model based on the second approach, a linear fractional transformation (LFT) based LPV controller synthesis approach is used to synthesize a controller [19]. However, the implementation of the designed LPV controllers requires the availability of all the scheduling variables, some of which are not measurable in the copolymerization reactor model. Therefore, an extended Kalman filter (EKF) [20] is designed for the nonlinear model of the copolymerization reactor in order to estimate its state vector. The aim of this paper is to emphasize the capability of the LPV controllers, designed on the basis of a reduced model, to provide high performance control of the polymerization reactor by enhancing the settling time of the output and reducing the control effort. A comparative study on the designed LPV controllers highlights the compromise between the design complexity and performance of the LPV controller on one hand, and the stability guarantee of the closed-loop with the nonlinear process on the other hand.

The paper is organized as follows. In Section 2, the nonlinear copolymerization reactor model is introduced. Then, an LPV representation of the copolymerization reactor model is derived in Section 3. First, a parameter set mapping-based method for reducing the scheduling variables is applied. Then, an LPV representation of a specific model reduction approach for the process is developed. In Section 4, an LPV controller is synthesized for each approach

produced model. Next, the estimation of state variables through the use of the extended Kalman filter is detailed. In Section 5, the performance of the synthesized EKF-based controllers is examined and discussions addressing different aspects of both approaches are presented. Finally, Section 6 concludes the paper.

Notation: The symmetric completion of a matrix is denoted by $*$, $\mathbf{ker}[\boldsymbol{X}]$ denotes the null-space of a matrix $\boldsymbol{X}$ and $\mathbf{diag}(\boldsymbol{X}, \boldsymbol{Y})$ represents a block diagonal matrix with diagonal blocks $\boldsymbol{X}, \boldsymbol{Y}$.

2. Copolymerization reactor model

Copolymerization is the process of uniting two or more different monomers together to produce a copolymer. In this study, two monomers are considered, monomer A is methyl methacrylate (MMA) and monomer B is vinyl acetate (VA). In addition, it is assumed that the solvent is benzene, the initiator is azobisisobutyronitrile (AIBN), the chain transfer agent is acetaldehyde and the inhibitor is m-dinitrobenzene (m-DNB). These ingredients are continuously added into a well-mixed tank (Fig. 1) where an inhibitor is considered as an impurity and a coolant flows through the reactor jacket to remove the liberated heat via polymerization. The polymer, solvent, unreacted monomers, initiator and chain transfer agent compose the outflow of the reactor. The model of the solution

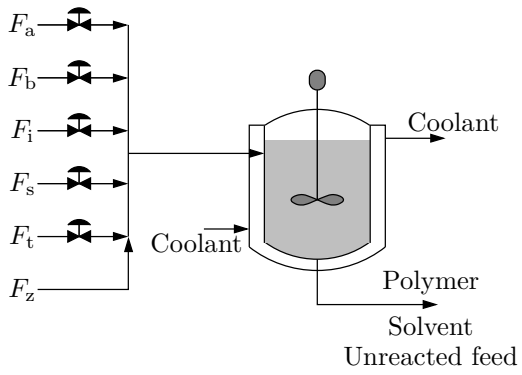

Figure 1: Copolymerization reactor

copolymerization reactor is based on a free radical mechanism [6] described with

the differential equations given as follows [3]:

$$
\begin{aligned}
\frac{\mathrm{d}C_k}{\mathrm{d}t} =& \frac{C_{k\mathrm{f}} - C_k}{\theta_\mathrm{r}} - R_k, \quad k = \mathrm{a}, \mathrm{b}, \mathrm{i}, \mathrm{s}, \mathrm{t}, \mathrm{z}, \\
\frac{\mathrm{d}T_\mathrm{r}}{\mathrm{d}t} =& \frac{T_\mathrm{rf} - T_\mathrm{r}}{\theta_\mathrm{r}} + \frac{(-\Delta H_\mathrm{paa})k_\mathrm{paa}C_\mathrm{a}C_\dot{\mathrm{a}} + (-\Delta H_\mathrm{pba})k_\mathrm{pba}C_\mathrm{a}C_\dot{\mathrm{b}}}{\rho_\mathrm{r}c_\mathrm{r}} \\
& + \frac{(-\Delta H_\mathrm{pab})k_\mathrm{pab}C_\mathrm{b}C_\dot{\mathrm{a}} + (-\Delta H_\mathrm{pbb})k_\mathrm{pbb}C_\mathrm{b}C_\dot{\mathrm{b}}}{\rho_\mathrm{r}c_\mathrm{r}} - \frac{U_\mathrm{r}S_\mathrm{r}(T_\mathrm{r} - T_\mathrm{j})}{V_\mathrm{r}\rho_\mathrm{r}c_\mathrm{r}}, \\
\frac{\mathrm{d}\lambda_\mathrm{a}}{\mathrm{d}t} =& \frac{-\lambda_\mathrm{a}}{\theta_\mathrm{r}} + R_\mathrm{a}, \\
\frac{\mathrm{d}\lambda_\mathrm{b}}{\mathrm{d}t} =& \frac{-\lambda_\mathrm{b}}{\theta_\mathrm{r}} + R_\mathrm{b}, \\
\frac{\mathrm{d}\psi_0^\mathrm{p}}{\mathrm{d}t} =& \frac{-\psi_0^\mathrm{p}}{\theta_\mathrm{r}} + \frac{1}{2}k_\mathrm{caa}(\psi_0^{\mathrm{a}\cdot})^2 + k_\mathrm{cab}\psi_0^{\mathrm{a}\cdot}\psi_0^{\mathrm{b}\cdot} + \frac{1}{2}k_\mathrm{cbb}(\psi_0^{\mathrm{b}\cdot})^2 + L_1\psi_0^{\mathrm{a}\cdot} + L_2\psi_0^{\mathrm{b}\cdot}, \\
\frac{\mathrm{d}\psi_1^\mathrm{p}}{\mathrm{d}t} =& \frac{-\psi_1^\mathrm{p}}{\theta_\mathrm{r}} + k_\mathrm{caa}\psi_0^{\mathrm{a}\cdot}\psi_1^{\mathrm{a}\cdot} + k_\mathrm{cab}(\psi_0^{\mathrm{a}\cdot}\psi_1^{\mathrm{b}\cdot} + \psi_0^{\mathrm{b}\cdot}\psi_1^{\mathrm{a}\cdot}) + k_\mathrm{cbb}\psi_0^{\mathrm{b}\cdot}\psi_1^{\mathrm{b}\cdot} + L_1\psi_1^{\mathrm{a}\cdot} + L_2\psi_1^{\mathrm{b}\cdot}, \\
\frac{\mathrm{d}\psi_2^\mathrm{p}}{\mathrm{d}t} =& \frac{-\psi_2^\mathrm{p}}{\theta_\mathrm{r}} + k_\mathrm{caa}\left\{(\psi_1^{\mathrm{a}\cdot})^2 + \psi_0^{\mathrm{a}\cdot}\psi_2^{\mathrm{a}\cdot}\right\} + k_\mathrm{cab}(2\psi_1^{\mathrm{a}\cdot}\psi_1^{\mathrm{b}\cdot} + \psi_2^{\mathrm{b}\cdot}\psi_0^{\mathrm{a}\cdot} + \psi_2^{\mathrm{a}\cdot}\psi_0^{\mathrm{b}\cdot}) \\
& + k_\mathrm{cbb}\left\{(\psi_1^{\mathrm{b}\cdot})^2 + \psi_0^{\mathrm{b}\cdot}\psi_2^{\mathrm{b}\cdot}\right\} + L_1\psi_2^{\mathrm{a}\cdot} + L_2\psi_2^{\mathrm{b}\cdot},
\end{aligned}
\tag{1}
$$

where $C_{k\mathrm{f}} = \frac{F_k}{Q_\mathrm{f}M_k}$, $Q_\mathrm{f} = \frac{\sum_k F_k}{\rho_\mathrm{r}}$, $\theta_\mathrm{r} = \frac{V_\mathrm{r}}{Q_\mathrm{f}}$, C_k is the concentration (kmol/m^3), M is the mole-cular weight (kg/kmol), Q is the volumetric flow rate (m^3/s), R is the reaction rate (kmol/m^3), S is the surface area (m^2), T is the temperature (K), U is the overall heat transfer coefficient (kJ/m^{2}s K), V is the volume (m^3), t is the time (s), θ is the residence time (s), λ is the molar concentration of monomer in polymer, ρ is the density (kg/m^3), and ψ_j is the j^{th} moment of molecular weight distribution. The sub and superscripts a, b, i, s, t, z, r, j, p, c are related to monomer A, monomer B, initiator, solvent, chain transfer, inhibitor, reactor, cooling jacket, dead polymer, and combination, respectively, and the superscript (.) represents the free radical. The values of the constant parameters are given in Table 1. For more details on the kinetic and the thermodynamic parameters (such as k_paa and ΔH_paa, respectively), as well as the calculation of the reaction rates R_k ($k = \mathrm{a}, \mathrm{b}, \mathrm{i}, \mathrm{s}, \mathrm{t}, \mathrm{z}$), the free radial concentrations $C_\dot{\mathrm{a}}, C_\dot{\mathrm{b}}$, and the moments $\psi^{\mathrm{a}\cdot}, \psi^{\mathrm{b}\cdot}$, interested reader is referred to [6] (Eqs. (1)-(12), Eqs. (31)-(36) and Table 7).

The inputs of the system (1) are the reactor flows F_a, F_b, F_i, F_s, F_t, F_z and the temperature of the reactor jacket T_j. The important reactor output variables for the product quality control are the reactor temperature T_r, the polymer production rate G_pi, the mole fraction of monomer A in the copolymer

Y_{ap}, and the average molecular weight M_{pw}. The output equations are

$$\begin{aligned} G_{\mathrm{pi}} &= (R_{\mathrm{a}} M_{\mathrm{a}} + R_{\mathrm{b}} M_{\mathrm{b}}) V_{\mathrm{r}}, \\ Y_{\mathrm{ap}} &= \tfrac{\lambda_{\mathrm{a}}}{\lambda_{\mathrm{a}}+\lambda_{\mathrm{b}}}, \\ M_{\mathrm{pw}} &= \tfrac{\psi_2^{\mathrm{p}}}{\psi_1^{\mathrm{p}}}. \end{aligned} \tag{2}$$

The nonlinear model of the reactor (1) was derived in [6] from the first principles of mass and energy balance and was validated on a real plant (see [21], [22], [23], [24] and [25]). Moreover, this model has been extensively used as a benchmark for copolymerization process control in the literature (see, e.g., [3], [4], [7], [26] and references therein). The main challenge of this high fidelity nonlinear copolymerization model is its volatile nonlinear behavior and extensive operating range, which makes it a challenging and highly relevant (from the practical perspective) application in industrial process control. In [6], the derived process control schemes have been successfully implemented and tested in several real-world plants. Furthermore, as explained in [26], the process model is given realistic measured disturbances based on experience with an industrial copolymerization process, thereby making the feedback control problem representative of the challenges faced by industrial practitioners.

The control objective considered in this paper is to ensure a fast transition between two steady-state operating points given in Table 2 while rejecting unmeasured input disturbance represented by F_{z}. The first operating point, OP1, given in [6] was obtained for a monomer feed ratio $F_{\mathrm{a}}/F_{\mathrm{b}} = 0.2$ while the second one, OP2, was obtained by increasing the ratio by 0.25 keeping F_{b} constant. It is worth mentioning that the solution copolymerization reactor is highly sensitive to changes in the monomer feed ratios, i.e., $F_{\mathrm{a}}/F_{\mathrm{b}}$ [3]. In order to achieve this objective, the manipulated variables to control the four previously specified output variables are chosen –based on the investigation in [6]– to be F_{a}, F_{b}, F_{t} and T_{j}. For comparison purposes, the same control objective and associated variables are considered whilst the other inputs are kept constant as $F_{\mathrm{i}} = 0.18$ (kg/h) and $F_{\mathrm{s}} = 36$ (kg/h) [3].

Table 1: Values for the constant parameters.

M_{a}	100.1 (kg/kmol)	S	4.6 (m^2)
M_{b}	86.09 (kg/kmol)	V	1 (m^3)
M_{i}	164 (kg/kmol)	U	6.0×10^{-2} ($\mathrm{kJ/m^2 s\,K}$)
M_{s}	78.11 (kg/kmol)	c	2.01 ($\mathrm{kJ/kg\,K}$)
M_{t}	44.05 (kg/kmol)	ρ	879 ($\mathrm{kJ/m^3}$)
M_{z}	168.11 (kg/kmol)	T_{rf}	353.0203 (K)

For the operating points considered in Table 2, it has been shown in [7] that

Table 2: Operating conditions.

	OP1	OP2
G_{pi} (kg/h)	23.35	24.9
Y_{ap}	0.56	0.64
M_{pw} (10^5 kg/kmol)	0.35	0.39
T_{r} (K)	353.06	353.3

closing the temperature loop with a PI controller, i.e., assigning the manipulated variable T_{j} to only control T_{r}, yields a well-conditioned system, which allows to fully exploit the compensation capabilities of multivariable controllers. Furthermore, safety is another reason for the justification of closing the temperature loop to prevent the reactor runaway. It is mentioned in [7] that a well-conditioned control problem has been obtained and "by closing the temperature loop, the complexity of the problem is not reduced, it is merely a structured approach to the control design". Consequently, the dynamics of T_{r} can be eliminated from the system (1), which reduces the number of states to 11.

3. Linear parameter-varying modeling of the copolymerization reactor

In this section, linear parameter-varying (LPV) representations of the nonlinear model of the copolymerization reactor are developed to hide the system nonlinearities in the LPV scheduling variables. While other methods for LPV modeling, like Jacobian linearization based approach or state transformation, tend to describe only certain aspects of the original nonlinear behavior, the direct transformation methods generate LPV models that can completely embed in their solution sets the behavior of the original nonlinear model [18]. In continuous time, the state-space representation of an LPV system with static dependency is described as

$$\begin{cases} \dot{\mathbf{x}}(\mathrm{t}) = \boldsymbol{A}(\boldsymbol{\theta}(\boldsymbol{t}))\boldsymbol{x}(\boldsymbol{t}) + \boldsymbol{B}(\boldsymbol{\theta}(\boldsymbol{t}))\boldsymbol{u}(\boldsymbol{t}), \\ \boldsymbol{y}(\boldsymbol{t}) = \boldsymbol{C}(\boldsymbol{\theta}(\boldsymbol{t}))\boldsymbol{x}(\boldsymbol{t}) + \boldsymbol{D}(\boldsymbol{\theta}(\boldsymbol{t}))\boldsymbol{u}(\boldsymbol{t}), \end{cases} \tag{3}$$

with the state vector $\boldsymbol{x}(\boldsymbol{t}) \in \mathbb{R}^n$, the input vector $\boldsymbol{u}(\boldsymbol{t}) \in \mathbb{R}^m$, the output vector $\boldsymbol{y}(\boldsymbol{t}) \in \mathbb{R}^p$ and the system matrices $\mathbf{A}, \mathbf{B}, \mathbf{C}$ and $\boldsymbol{D}$ being continuous matrix functions of the scheduling variable vector $\boldsymbol{\theta}(\boldsymbol{t}) \in \mathbb{R}^l$. $\boldsymbol{\theta}(\boldsymbol{t})$ depends on a vector of measurable signals $\boldsymbol{\rho}(\boldsymbol{t}) \in \mathbb{R}^k$ in the modeled system, according to $\boldsymbol{\theta}(\boldsymbol{t}) = \boldsymbol{q}(\boldsymbol{\rho}(\boldsymbol{t}))$, where $\boldsymbol{q}$ is a bounded function. The variable $\boldsymbol{\theta}(\boldsymbol{t})$ is defined over a compact scheduling set $\mathbb{P}_\theta \subset \mathbb{R}^l$ such that $\boldsymbol{\theta}(\boldsymbol{t}) : \mathbb{R}^l \to \mathbb{P}_\theta$ and $\mathbb{P}_\theta$ is often considered as a polytope and defined as the convex hull given by the vertices $\boldsymbol{\theta}_{\mathbf{v}_i}$ such that

$$\mathbb{P}_\theta := \mathrm{Co}\{\boldsymbol{\theta}_{\mathbf{v_1}}, \boldsymbol{\theta}_{\mathbf{v_2}}, ..., \boldsymbol{\theta}_{\mathbf{v_L}}\}, \tag{4}$$

where $L = 2^l$ and $\mathrm{Co}\{\cdot\}$ denotes a convex hull. The LPV representation (3) is called affine in scheduling dependence if the state-space matrices depend affinely on $\boldsymbol{\theta}$ as

$$\boldsymbol{M}(\boldsymbol{\theta}) = \boldsymbol{M_0} + \sum_{i=1}^{l} \theta_i \boldsymbol{M_i}, \tag{5}$$

where θ_i is the i^{th} element of $\boldsymbol{\theta}$. Since $\boldsymbol{\theta}$ can be expressed as a convex combination of L vertices $\boldsymbol{\theta}_{\mathbf{v_i}}$, the system can be represented by a linear combination of LTI models at the vertices. The resulting LPV representation is thus called polytopic where each matrix is represented as

$$\boldsymbol{Q}(\boldsymbol{\theta}) = \sum_{i=1}^{L} \alpha_i \boldsymbol{Q}(\boldsymbol{\theta}_{\mathbf{v_i}}), \tag{6}$$

such that $\sum_{i=1}^{L} \alpha_i = 1$ with $\alpha_i \geq 0$.

3.1. Full LPV model of the copolymerization reactor

Eliminating the dynamics of T_r from (1) results in a nonlinear model with the state vector $\boldsymbol{x} = [C_\mathrm{a}\, C_\mathrm{b}\, C_\mathrm{i}\, C_\mathrm{s}\, C_\mathrm{t}\, C_\mathrm{z}\, \lambda_\mathrm{a}\, \lambda_\mathrm{b}\, \psi_0^\mathrm{p}\, \psi_1^\mathrm{p}\, \psi_2^\mathrm{p}]^\top$, the output vector $\boldsymbol{y} = [G_\mathrm{pi}\, Y_\mathrm{ap}\, M_\mathrm{pw}]^\top$ and the full input vector $\boldsymbol{u} = [F_\mathrm{a}\, F_\mathrm{b}\, F_\mathrm{i}\, F_\mathrm{s}\, F_\mathrm{t}\, F_\mathrm{z}]^\top$. The nonlinear model (1) can be represented in the LPV form (3) with the state-space matrices as

$$\boldsymbol{A}(\boldsymbol{\theta}) = \begin{bmatrix}
-\theta_1-\theta_2 & 0 & 0 & 0 & 0 & 0 & 0 & 0 & 0 & 0 & 0 \\
0 & -\theta_1-\theta_3 & 0 & 0 & 0 & 0 & 0 & 0 & 0 & 0 & 0 \\
0 & 0 & -\theta_1-\theta_4 & 0 & 0 & 0 & 0 & 0 & 0 & 0 & 0 \\
0 & 0 & 0 & -\theta_1-\theta_5 & 0 & 0 & 0 & 0 & 0 & 0 & 0 \\
0 & 0 & 0 & 0 & -\theta_1-\theta_6 & 0 & 0 & 0 & 0 & 0 & 0 \\
0 & 0 & 0 & 0 & 0 & -\theta_1-\theta_7 & 0 & 0 & 0 & 0 & 0 \\
\theta_2 & 0 & 0 & 0 & 0 & 0 & -\theta_1 & 0 & 0 & 0 & 0 \\
0 & \theta_3 & 0 & 0 & 0 & 0 & 0 & -\theta_1 & 0 & 0 & 0 \\
\theta_8 & \theta_9 & 0 & 0 & 0 & 0 & 0 & 0 & -\theta_1 & 0 & 0 \\
\theta_{10} & \theta_{11} & 0 & 0 & 0 & 0 & 0 & 0 & 0 & -\theta_1 & 0 \\
\theta_{12} & \theta_{13} & 0 & 0 & 0 & 0 & 0 & 0 & 0 & 0 & -\theta_1
\end{bmatrix},$$

$$\boldsymbol{B}(\boldsymbol{\theta}) = \begin{bmatrix}
\frac{1}{M_\mathrm{a}V_\mathrm{r}} & 0 & 0 & 0 & & \\
0 & \frac{1}{M_\mathrm{b}V_\mathrm{r}} & 0 & 0 & 0 & 0 \\
0 & 0 & \frac{1}{M_\mathrm{i}V_\mathrm{r}} & 0 & 0 & 0 \\
0 & 0 & 0 & \frac{1}{M_\mathrm{s}V_\mathrm{r}} & 0 & 0 \\
0 & 0 & 0 & 0 & \frac{1}{M_\mathrm{t}V_\mathrm{r}} & 0 \\
0 & 0 & 0 & 0 & 0 & \frac{1}{M_\mathrm{z}V_\mathrm{r}} \\
0 & 0 & 0 & 0 & 0 & 0 \\
0 & 0 & 0 & 0 & 0 & 0 \\
0 & 0 & 0 & 0 & 0 & 0 \\
0 & 0 & 0 & 0 & 0 & 0 \\
0 & 0 & 0 & 0 & 0 & 0
\end{bmatrix}, \boldsymbol{C}(\boldsymbol{\theta}) = \begin{bmatrix}
0 & 0 & 0\,0\,0\,0 & 0 & 0\,0\,0\,\theta_{14} \\
0 & 0 & 0\,0\,0\,0 & \theta_{15} & 0\,0\,0 & 0 \\
M_\mathrm{a}V_\mathrm{r}\theta_2 & M_\mathrm{b}V_\mathrm{r}\theta_3 & 0\,0\,0\,0 & 0 & 0\,0\,0 & 0
\end{bmatrix}, \boldsymbol{D}(\boldsymbol{\theta}) = \mathbb{O}_{\mathbf{3\times 6}}. \tag{7}$$

The scheduling variable $\boldsymbol{\theta(t)} \in \mathbb{R}^{15}$, as defined in the Appendix, is a vector of complicated functions that depend on the input and the state vectors used to construct the measured signals in $\boldsymbol{\rho(t)}$ as

$$\boldsymbol{\rho} = \left[F_\mathrm{a}\, F_\mathrm{b}\, F_\mathrm{i}\, F_\mathrm{s}\, F_\mathrm{t}\, F_\mathrm{z}\, C_\mathrm{a}\, C_\mathrm{b}\, C_\mathrm{i}\, C_\mathrm{s}\, C_\mathrm{t}\, C_\mathrm{z}\, T_\mathrm{r}\, \lambda_\mathrm{a}\, \lambda_\mathrm{b}\, \psi_1\right]^\top. \tag{8}$$

The scheduling set $\mathbb{P}_\theta$ can be defined by obtaining bounds on $\boldsymbol{\theta}$ based on operational limits of $\boldsymbol{\rho}$, which can be computed according to the operating region defined in Table 2 as follows: First, one chooses an initial range for the inputs and refers to such range as the *input range*. Then, a set of grid points is produced for the input range; these points can then be used to generate a set of operating points by computing the corresponding steady-state values of the state vector of (1), such that the operating points defined in Table 2 are covered. Finally, the bounds of $\boldsymbol{\theta}$, and hence, $\mathbb{P}_\theta$ (see (4)) can be defined. The input range can be redefined after the control synthesis step according to the closed-loop operation. It turns out that for the operating region (Table 2), the input range

$$\begin{aligned} 18 \leq F_{\mathrm{a}} &\leq 22.5 \text{ kg/h}, \\ 87 \leq F_{\mathrm{b}} &\leq 93 \text{ kg/h}, \\ 1 \leq F_{\mathrm{t}} &\leq 4 \text{ kg/h}, \\ F_{\mathrm{i}} &= 0.18 \text{ kg/h}, \\ F_{\mathrm{s}} &= 36 \text{ kg/h} \end{aligned} \tag{9}$$

is sufficient to define $\mathbb{P}_\theta$. In the following the full LPV model is referred to as $\mathcal{M}_\theta$.

Using the full LPV model $\mathcal{M}_\theta$ could be too complex for LPV control synthesis to achieve a specific desired control performance due to the large number of scheduling variables $l = 15$. Based on the observations reported in [16], the large number of scheduling variables renders the synthesis problem intractable due to the large number of underlying matrix inequalities [8] or decision variables [19]. Furthermore, even if rendered tractable in the linear fractional transformation (LFT) framework, the necessary structural constraints, e.g., defining structure for so-called multipliers or scalings commonly used in LFT synthesis framework [19], may render the resulting control performance overly conservative. Finally, online controller implementation may turn out to be excessively costly. Therefore, the number of scheduling variables is reduced by means of two different techniques described in the following sections. In the first method, the parameter set mapping (PSM) method results in an approximate LPV model with reduced number of scheduling variables, whereas, in the second one, reformulating the nonlinear model allows to reduce the number of scheduling variables while preserving the input-output behavior of the initial process.

3.2. Reduced LPV modeling via parameter set mapping

The parameter set mapping can allow to develop an approximate LPV model of the original LPV model with fewer scheduling variables. For LPV models with affine dependence on the scheduling variables, PSM exploits the correlation of the variables and neglects the "less significant" directions in the mapped space. Hence, it allows to obtain a lower dimension and tighter range of variation of the scheduling variables and possibly reduce the conservatism of the overall modeling concept. The PSM can allow a trade-off between the number of scheduling variables and the desired model accuracy [15, 18].

For the sake of completeness, the PSM procedure is reviewed next. Given the LPV model (3), the LPV model reduction problem is to find a mapping $\boldsymbol{\phi(t)} = \boldsymbol{h(\theta(t))}$, $\boldsymbol{h} : \mathbb{R}^k \to \mathbb{R}^m$, where $m < l$, such that an approximation of the LPV model (3) is obtained as

$$\begin{cases} \dot{\boldsymbol{x}}_{\mathbf{PSM}}(\boldsymbol{t}) = \hat{\boldsymbol{A}}(\boldsymbol{\phi(t)})\boldsymbol{x}_{\mathbf{PSM}}(\boldsymbol{t}) + \hat{\boldsymbol{B}}(\boldsymbol{\phi(t)})\boldsymbol{u(t)}, \\ \quad \boldsymbol{y(t)} = \hat{\boldsymbol{C}}(\boldsymbol{\phi(t)})\boldsymbol{x}_{\mathbf{PSM}}(\boldsymbol{t}) + \hat{\boldsymbol{D}}(\boldsymbol{\phi(t)})\boldsymbol{u(t)}. \end{cases} \tag{10}$$

The use of PSM procedure for LPV model reduction involves the following steps [15, 18]:

1. Obtain typical trajectories of the scheduling variables, from either measurements or simulations that cover the expected range of system operation. These trajectories are collected in a matrix $\boldsymbol{\Theta} \in \mathbb{R}^{l \times N}$ by sampling the scheduling variables at time instants $t = kT$, $(k = 0, 1, ..., N-1)$ with $N \gg l$, or by determining steady-state values of the scheduling variables related to a gridded operating regime.

2. In order to weight the elements of $\boldsymbol{\Theta}$ equally, a normalization is required. The rows $\boldsymbol{\Theta_i}$ of the data matrix $\boldsymbol{\Theta}$ are normalized such that

$$\boldsymbol{\Theta}_{\boldsymbol{i}}^{\mathbf{n}} = \mathcal{N}(\boldsymbol{\Theta}_{\boldsymbol{i}}), \quad \text{with} \quad \bar{\Theta}_i^{\mathrm{n}} = 0, \quad \sigma_i^{\mathrm{n}} = \sqrt{\mathrm{Var}\{\boldsymbol{\Theta}_{\boldsymbol{i}}^{\mathbf{n}}\}} = 1,$$

where $\mathcal{N}$ denotes row-wise scaling to achieve zero mean data with one standard deviation, $\bar{\Theta}_i^{\mathrm{n}}$ is the sample mean value of $\boldsymbol{\Theta}_{\boldsymbol{i}}^{\mathbf{n}}$ and σ_i^{n} is the sample standard deviation of $\boldsymbol{\Theta}_{\boldsymbol{i}}^{\mathbf{n}}$. The normalized data matrix $\boldsymbol{\Theta}^{\mathbf{n}} \in \mathbb{R}^{l \times N}$ is given by:

$$\boldsymbol{\Theta}^{\mathbf{n}} = \boldsymbol{\mathcal{N}(\Theta)}. \tag{11}$$

3. The PCA method is then applied to the normalized matrix $\boldsymbol{\Theta}^{\mathbf{n}}$ in (11) in order to find a mapped parameter set with most significant information contained in the data. *Singular value decomposition* (SVD) is used to deduce an orthogonal set of basis vectors to $\boldsymbol{\Theta}^{\mathbf{n}}$ such that

$$\hat{\boldsymbol{\Theta}}^{\mathbf{n}} = \boldsymbol{U}_{\mathbf{s}}\boldsymbol{\Sigma}_{\mathbf{s}}\boldsymbol{V}_{\mathbf{s}}^{\top} = \boldsymbol{U}_{\mathbf{s}}\boldsymbol{\Phi}, \tag{12}$$

where the first m significant singular values are selected in $\boldsymbol{\Sigma}_{\mathbf{s}}$, and the unitary matrix $\boldsymbol{U}_{\mathbf{s}} \in \mathbb{R}^{l \times m}$ represents the basis of the significant column space of $\boldsymbol{\Theta}^{\mathbf{n}}$.

4. The key idea of using PSM as proposed in [18] is to apply the normalized mapping $\boldsymbol{U}_{\mathbf{s}}$ to determine a parameter function that defines the reduced LPV representation. More specifically, the reduced scheduling variable $\boldsymbol{\phi(t)}$ will be defined via

$$\boldsymbol{\Phi} = \boldsymbol{U}_{\mathbf{s}}^{\top}\hat{\boldsymbol{\Theta}}^{\mathbf{n}} \;\Leftrightarrow\; \boldsymbol{\phi(t)} = \boldsymbol{U}_{\mathbf{s}}^{\top}\boldsymbol{\mathcal{N}(\theta(t))}. \tag{13}$$

Thus, the mappings $\hat{\boldsymbol{A}}, \hat{\boldsymbol{B}}, \hat{\boldsymbol{C}}, \hat{\boldsymbol{D}}$ in (10) are related to the new scheduling vari-

ables $\hat{\boldsymbol{\theta}}(\boldsymbol{t})$ by [18],

$$\begin{bmatrix} \hat{\boldsymbol{A}}(\boldsymbol{\phi(t)})\ \hat{\boldsymbol{B}}(\boldsymbol{\phi(t)}) \\ \hat{\boldsymbol{C}}(\boldsymbol{\phi(t)})\ \hat{\boldsymbol{D}}(\boldsymbol{\phi(t)}) \end{bmatrix} = \begin{bmatrix} \boldsymbol{A}(\hat{\boldsymbol{\theta}}(\boldsymbol{t}))\ \boldsymbol{B}(\hat{\boldsymbol{\theta}}(\boldsymbol{t})) \\ \boldsymbol{C}(\hat{\boldsymbol{\theta}}(\boldsymbol{t}))\ \boldsymbol{D}(\hat{\boldsymbol{\theta}}(\boldsymbol{t})) \end{bmatrix}, \tag{14}$$

where the vector $\hat{\boldsymbol{\theta}}(\boldsymbol{t})$ is defined by

$$\hat{\boldsymbol{\theta}}(\boldsymbol{t}) = \boldsymbol{\mathcal{N}^{-1}}\left(\boldsymbol{U_s}\boldsymbol{\phi(t)}\right), \tag{15}$$

and $\boldsymbol{\mathcal{N}^{-1}}$ denotes row-wise rescaling. Each element of $\hat{\boldsymbol{\theta}}(\boldsymbol{t})$ is determined as $\hat{\theta}_i(t) = \bar{\Theta}_i + \sigma_i \left(\boldsymbol{U_s}\boldsymbol{\phi(t)}\right)_i$, where $\bar{\Theta}_i$ and σ_i represent the mean and the standard deviation of the rows of the data matrix $\boldsymbol{\Theta}$, respectively. Since the LPV model (3) is affine in $\boldsymbol{\theta}$, each matrix in (14) is described as

$$\hat{\boldsymbol{Q}}(\boldsymbol{\phi(t)}) = \boldsymbol{Q}(\hat{\boldsymbol{\theta}}(\boldsymbol{t})) = \boldsymbol{Q_0} + \sum_{i=1}^{l} \boldsymbol{Q_i}\, \hat{\theta}_i(t), \tag{16}$$

which leads to

$$\begin{aligned} \hat{\boldsymbol{Q}}(\boldsymbol{\phi(t)}) &= \boldsymbol{Q_0} + \textstyle\sum_{i=1}^{l} \boldsymbol{Q_i}\, \bar{\Theta}_i + \sum_{i=1}^{l} \boldsymbol{Q_i}\, \sigma_i \left(\boldsymbol{U_s}\boldsymbol{\phi(t)}\right)_i \\ &= \underbrace{\boldsymbol{Q_0} + \sum_{i=1}^{l} \boldsymbol{Q_i}\, \bar{\Theta}_i}_{\hat{\boldsymbol{Q}}_{\boldsymbol{0}}} + \textstyle\sum_{j=1}^{m} \underbrace{\sum_{i=1}^{l} \boldsymbol{Q_i}\, \sigma_i \left(\boldsymbol{U_s}\right)_{i,j}}_{\hat{\boldsymbol{Q}}_{\boldsymbol{j}}}\, \phi_j(t) \\ &= \hat{\boldsymbol{Q}}_{\boldsymbol{0}} + \textstyle\sum_{j=1}^{m} \hat{\boldsymbol{Q}}_{\boldsymbol{j}}\, \phi_j(t) \end{aligned} \tag{17}$$

where $\left(\boldsymbol{U_s}\right)_{i,j}$ represents the $(i,j)^{\text{th}}$ component of the matrix $\boldsymbol{U_s}$. This proves that the reduced model is also affine in the reduced scheduling variable $\boldsymbol{\phi(t)}$.

At any given time, the mapped vector $\boldsymbol{\phi(t)}$ is computed from (13), which is used to generate the scheduling variable $\hat{\boldsymbol{\theta}}(\boldsymbol{t})$ from (15) and then implemented in the original LPV model (3). This leads to a reduced LPV model that depends on the new scheduling variable $\hat{\boldsymbol{\theta}}(\boldsymbol{t})$ [18].

Next, the PSM technique is applied to the LPV model $\mathcal{M}_\theta$. Here the matrix $\boldsymbol{\Theta}$ is defined based on steady-state values of the scheduling variables corresponding to grid points in the scheduling signal range that had been used to define $\mathbb{P}_\theta$. Then, $\boldsymbol{\Sigma_s}$ from (12) is obtained as

$$\begin{aligned} \boldsymbol{\Sigma_s} = \operatorname{diag}\big(&14.23,\ 12.2,\ 6.01,\ 1.36,\ 0.58,\ 0.27,\ 0.08,\ 0.03,\ 0.01, \\ &5\times10^{-3},\ 2\times10^{-3},\ 10^{-3},\ 6\times10^{-4},\ 10^{-5},\ 10^{-6}\big). \end{aligned} \tag{18}$$

According to the scheduling dimension considered, the matrix $\boldsymbol{U_s}$ is calculated from (12) and then used for the online calculation of $\boldsymbol{\phi(t)}$ in (13) and $\hat{\boldsymbol{\theta}}(\boldsymbol{t})$ in (15). For the transition from OP1 to OP2 as shown in Table 2, the reduced

LPV model provided by the PSM method is simulated with various scheduling dimensions $m = 1, 2, 3$, since the first three singular values of the matrix $\mathbf{\Sigma_s}$ in (18) are the most significant ones. The end result of this simplification is a projection matrix which projects the old measured variables to a new set of variables. Therefore, unlike the balanced truncation method in the LTI case, it is not possible to explicitly deduce which variables have been neglected. PSM projects the scheduling variables range of an LPV model to another set with smaller dimension, which results in an LPV representation with a reduced number of the scheduling variables. The best fit rate (BFR) of the state evolution between the original state vector $\boldsymbol{x}$ obtained from (1) and the state vector of the scheduling dimension reduced LPV model $\boldsymbol{x_{PSM}}$ obtained from (10) is calculated as

$$\text{BFR} = 100\% \times \max\left(1 - \frac{||\boldsymbol{x} - \boldsymbol{x_{PSM}}||_2}{||\boldsymbol{x} - \bar{x}||_2}, 0\right), \tag{19}$$

where $\bar{x}$ is the sample mean of $\boldsymbol{x}$, and $||.||_2$ is the ℓ_2 norm. The relative accuracy, which is an indicator of the quality of the reduced LPV model by PSM, is defined as

$$r_{\text{a}} = \frac{\sum_{i=1}^{m} \sigma_i^2}{\sum_{i=1}^{15} \sigma_i^2},$$

where σ_i denotes the i^{th} singular value of the matrix $\mathbf{\Sigma_s}$ in (18) and is presented in Table 3. Despite its low accuracy, the reduced LPV model with scheduling dimension of $m = 1$ is considered for synthesizing LPV controller for the copolymerization reactor as it yields minimal complexity. Furthermore, the LPV controller designed based on the reduced LPV model with $m = 1$ shows a better closed-loop performance in terms of the lower convergence time and less overshoots of the outputs compared to the reduced models with scheduling dimensions of $m = 2$ and $m = 3$. As discussed in [18], the potential benefit of a tighter set of scheduling variables might not necessarily complicate the controller synthesis and may even lead to a better closed-loop performance. In the sequel, this reduced model is referred to as $\mathcal{M}_\phi$. The new scheduling variable $\boldsymbol{\phi(t)}$ is defined in a new scheduling set $\mathbb{P}_\phi \subset \mathbb{R}^m$, which is the convex hull of the vertices $\boldsymbol{\phi_{\mathbf{v}_i}}$ as in (4).

Table 3: Accuracy and BFR corresponding to the LPV models with reduced scheduling dimensions.

	Accuracy (%)	BFR (%)
$m = 1$	55	77.8
$m = 2$	90.1	82.4
$m = 3$	99.4	96.5

3.3. LPV modeling based on the reformulated nonlinear model

The LPV model $\mathcal{M}_\phi$ derived in the previous section provides an approximation of the original nonlinear model. Therefore, the stability and performance

guarantees are rendered void if the designed controller, based on such approximate model, is implemented on the original plant. In some cases, a posteriori analysis should be performed on the full model to assess – and if applicable to recover – these guarantees, see [27] and [28] for more details. To avoid such analysis, next, the representation of the nonlinear model (1) is reformulated in order to produce, for control synthesis, a reduced complexity LPV model, in terms of the number of scheduling variables, that can preserve the same input-output behavior of the nonlinear model in a prespecified range of operation. Consequently, at the expense of some conservatism, controllers based on such model guarantee stability and performance when implemented on the original plant. Again, the nonlinear model (1) is considered after closing the temperature loop. The idea of reformulating the nonlinear model is based on truncating those states that do not explicitly affect the outputs of the model. Using (2), it can be seen that the three outputs of the model are directly affected by the states $C_\mathrm{a}, C_\mathrm{b}, \lambda_\mathrm{a}, \psi_2$. Therefore, the remaining states of the original model can be truncated, and hence, the following reduced model can be obtained

$$\begin{aligned}
\frac{\mathrm{d}}{\mathrm{d}t}C_\mathrm{a} &= -\theta_2 C_\mathrm{a} + \frac{F_\mathrm{a}}{M_\mathrm{a}V} - \frac{F_\mathrm{isz}}{V\rho}C_\mathrm{a} - \frac{(F_\mathrm{a}+F_\mathrm{b}+F_\mathrm{t})}{V\rho}C_\mathrm{a},\\
\frac{\mathrm{d}}{\mathrm{d}t}C_\mathrm{b} &= -\theta_3 C_\mathrm{b} + \frac{F_\mathrm{b}}{M_\mathrm{b}V} - \frac{F_\mathrm{isz}}{V\rho}C_\mathrm{b} - \frac{(F_\mathrm{a}+F_\mathrm{b}+F_\mathrm{t})}{V\rho}C_\mathrm{b},\\
\frac{\mathrm{d}}{\mathrm{d}t}\lambda_\mathrm{a} &= \theta_2 C_\mathrm{a} - \frac{F_\mathrm{isz}}{V\rho}\lambda_\mathrm{a} - \frac{(F_\mathrm{a}+F_\mathrm{b}+F_\mathrm{t})}{V\rho}\lambda_\mathrm{a},\\
\frac{\mathrm{d}}{\mathrm{d}t}\psi_2 &= \tilde{\theta}_{12} C_\mathrm{a} - \frac{F_\mathrm{isz}}{V\rho}\psi_2 - \frac{(F_\mathrm{a}+F_\mathrm{b}+F_\mathrm{t})}{V\rho}\psi_2,
\end{aligned} \tag{20}$$

with the outputs in (2), where

$$\tilde{\theta}_{12} = \frac{\theta_{12}C_\mathrm{a} + \theta_{13}C_\mathrm{b}}{C_\mathrm{a}}, \tag{21}$$

and $F_\mathrm{isz} = F_\mathrm{i} + F_\mathrm{s} + F_\mathrm{z}$, which is assumed to be a constant parameter[1] as it is composed of non-manipulated variables. Due to the variations of F_i, F_s and F_z during operation, these three reactor flows are considered to be unmeasured disturbances. In (21), $C_\mathrm{a} = 0$ is prohibitive[2] since it is meaningless to have zero concentration of polymer A, and hence, (21) remains bounded in the operational regime. The reformulated nonlinear model (20) with (2) depends on the variables θ_2, θ_3, $\tilde{\theta}_{12}$, θ_{13} and θ_{15} which are functions of all states of the system. In simulation, the reformulated nonlinear model (20) should receive all the truncated states from the system to be able to compute θ_2, θ_3, $\tilde{\theta}_{12}$, θ_{13} and θ_{15}, see Figure 2. In this sense, the reformulated model can preserve the same input-output behavior of the original one. Note that an LPV controller based

[1] It is possible to consider F_isz time-varying at the expense of increasing model complexity.

[2] It is possible to consider $\tilde{\theta}_{13} = \frac{\theta_{12}C_\mathrm{a}+\theta_{13}C_\mathrm{b}}{C_\mathrm{b}}$ instead (as $C_\mathrm{b} = 0$ is also prohibitive).

on such reformulated model should receive all the states of the system in order to compute the scheduling variable $\boldsymbol{\theta}$.

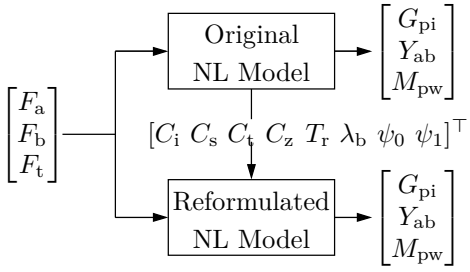

Figure 2: Open-loop simulation of the reformulated nonlinear model

Now, an exact LPV representation for (1) with (2) can be written in the form (3) where the state matrices are given by

$$
\begin{aligned}
\boldsymbol{A}(\boldsymbol{\theta}) &= \begin{bmatrix} -(\theta_2 + \frac{F_\mathrm{isz}}{V\rho}) & 0 & 0 & 0 \\ 0 & -(\theta_3 + \frac{F_\mathrm{isz}}{V\rho}) & 0 & 0 \\ \theta_2 & 0 & -\frac{\sum_k F_k}{V\rho} & 0 \\ \tilde{\theta}_{12} & 0 & 0 & -\frac{F_\mathrm{isz}}{V\rho} \end{bmatrix}, \\
\boldsymbol{B}(\boldsymbol{\theta}) &= \begin{bmatrix} \frac{1}{M_\mathrm{a}V} - \frac{C_\mathrm{a}}{V\rho} & -\frac{C_\mathrm{a}}{V\rho} & -\frac{C_\mathrm{a}}{V\rho} \\ -\frac{C_\mathrm{b}}{V\rho} & \frac{1}{M_\mathrm{b}V} - \frac{C_\mathrm{b}}{V\rho} & -\frac{C_\mathrm{b}}{V\rho} \\ 0 & 0 & 0 \\ -\frac{\psi_2}{V\rho} & -\frac{\psi_2}{V\rho} & -\frac{\psi_2}{V\rho} \end{bmatrix}, \\
\boldsymbol{C}(\boldsymbol{\theta}) &= \begin{bmatrix} M_\mathrm{a}V\theta_2 & M_\mathrm{b}V\theta_3 & 0 & 0 \\ 0 & 0 & \theta_{15} & 0 \\ 0 & 0 & 0 & \theta_{14} \end{bmatrix}, \qquad \boldsymbol{D} = \boldsymbol{0},
\end{aligned}
\tag{22}
$$

where $\sum_k F_k = F_\mathrm{isz} + F_\mathrm{a} + F_\mathrm{b} + F_\mathrm{c}$. Note that for the representation (22), the functions $\theta_2, \theta_3, \tilde{\theta}_{12}, \theta_{15}, \theta_{14}$ and the states $C_\mathrm{a}, C_\mathrm{b}, \psi_2$ define the scheduling variables, resulting in a total of 8 scheduling variables. Next, this dimension is further reduced by introducing a new input vector

$$
\begin{bmatrix} u_1 \\ u_2 \\ u_3 \end{bmatrix} = \underbrace{\begin{bmatrix} \frac{1}{M_\mathrm{a}V} - \frac{C_\mathrm{a}}{V\rho} & -\frac{C_\mathrm{a}}{V\rho} & -\frac{C_\mathrm{a}}{V\rho} \\ -\frac{C_\mathrm{b}}{V\rho} & \frac{1}{M_\mathrm{b}V} - \frac{C_\mathrm{b}}{V\rho} & -\frac{C_\mathrm{b}}{V\rho} \\ -\frac{\psi_2}{V\rho} & -\frac{\psi_2}{V\rho} & -\frac{\psi_2}{V\rho} \end{bmatrix}}_{\boldsymbol{\mathcal{E}}} \begin{bmatrix} F_\mathrm{a} \\ F_\mathrm{b} \\ F_\mathrm{t} \end{bmatrix}. \tag{23}
$$

The transformation matrix $\boldsymbol{\mathcal{E}}$ in (23) is non-singular for all values of C_a, C_b and ψ_2 in the specified operating range. Then, a new constant matrix $\boldsymbol{B}$ for the

LPV model can be introduced as

$$\boldsymbol{\mathcal{B}} = \begin{bmatrix} 1 & 0 & 0 \\ 0 & 1 & 0 \\ 0 & 0 & 0 \\ 0 & 0 & 1 \end{bmatrix}, \tag{24}$$

in terms of the new input vector (23) considered for the model. Moreover, the new set of outputs is defined as

$$\begin{aligned} y_1 &= G_{\mathrm{pi}}, \\ y_2 &= Y_{\mathrm{ap}}/\theta_{15} = Y_{\mathrm{ap}}(\lambda_{\mathrm{a}} + \lambda_{\mathrm{b}}), \\ y_3 &= M_{\mathrm{pw}}/\theta_{14} = M_{\mathrm{pw}}\psi_1, \end{aligned} \tag{25}$$

and hence, the new $\boldsymbol{C}$ matrix for the model can be introduced as

$$\boldsymbol{\mathcal{C}}(\boldsymbol{\theta}) = \begin{bmatrix} M_{\mathrm{a}}V\theta_2 & M_{\mathrm{b}}V\theta_3 & 0 & 0 \\ 0 & 0 & 1 & 0 \\ 0 & 0 & 0 & 1 \end{bmatrix}. \tag{26}$$

Introducing the new inputs and outputs results in the LPV representation (3) of relatively low complexity for the nonlinear model. The new state-space matrices in terms of the scheduling variable $\boldsymbol{\zeta}$ are given by

$$\begin{aligned} \boldsymbol{\mathcal{A}}(\boldsymbol{\zeta}) &= \begin{bmatrix} -(\zeta_1 + \frac{F_{\mathrm{isz}}}{V\rho}) & 0 & 0 & 0 \\ 0 & -(\zeta_2 + \frac{F_{\mathrm{isz}}}{V\rho}) & 0 & 0 \\ \zeta_1 & 0 & -(\frac{\zeta_4}{V\rho} + \frac{F_{\mathrm{isz}}}{V\rho}) & 0 \\ \zeta_3 & 0 & 0 & -\frac{F_{\mathrm{isz}}}{V\rho} \end{bmatrix}, \\ \boldsymbol{\mathcal{B}} &\text{ in (24)}, \\ \boldsymbol{\mathcal{C}}(\boldsymbol{\zeta}) &= \begin{bmatrix} M_{\mathrm{a}}V\zeta_1 & M_{\mathrm{b}}V\zeta_2 & 0 & 0 \\ 0 & 0 & 1 & 0 \\ 0 & 0 & 0 & 1 \end{bmatrix}, \text{ and } \boldsymbol{\mathcal{D}} = \mathbf{0}, \end{aligned} \tag{27}$$

where $\zeta_1 = \theta_2$, $\zeta_2 = \theta_3$, $\zeta_3 = \tilde{\theta}_{12}$, $\zeta_4 = F_{\mathrm{a}} + F_{\mathrm{b}} + F_{\mathrm{t}}$ and $\zeta_1, \cdots, \zeta_4$ are the elements of the entries of the scheduling vector $\boldsymbol{\zeta}$. Taking into consideration (23) and (25), the LPV representation (3) with (27) has the same input-output map as that of the nonlinear model (1) as long as the LPV model receives the truncated states from the nonlinear model as shown in Figure 2. Note that ζ_i are functions of the preserved variables collected in $\boldsymbol{\rho}$ as described by (8). Based

on the input range defined in (9), the bounds of $\boldsymbol{\zeta}$ are

$$\begin{aligned} 0.1618 \leq \zeta_1 \leq 0.1771, \\ 0.4823 \leq \zeta_2 \leq 0.5861, \\ 0.0170 \leq \zeta_3 \leq 0.0202, \\ 2.6124 \leq \zeta_4 \leq 4.0512, \end{aligned} \tag{28}$$

which can be used to define a new compact parameter set $\mathbb{P}_\zeta$. In the sequel, the LPV model (3) with (27) is referred to as $\mathcal{M}_\zeta$.

The resulted low complexity LPV model, $\mathcal{M}_\zeta$, in terms of the dynamical order and scheduling dimension guarantees the stability and desired performance for the original nonlinear model. However, losing the dynamical effects of the truncated states in $\mathcal{M}_\zeta$ might limit the achievable performance of such controllers without affecting the closed-loop stability, provided that all the scheduling variables are confined within their prespecified bounds (see Section 4.2).

4. LPV control synthesis

In this section, the control synthesis approaches proposed in [8] and [19] are utilized to design LPV controllers based on $\mathcal{M}_\phi$ and $\mathcal{M}_\zeta$, respectively. The LPV model $\mathcal{M}_\phi$ has just one scheduling variable, whereas $\mathcal{M}_\zeta$ has 4 scheduling variables, which is relatively large. Therefore, the linear fractional transformation (LFT) gain-scheduling approach [19] is adopted to design the LPV controller for $\mathcal{M}_\zeta$. This approach provides a versatile LPV controller synthesis framework capable of handling plants with relatively large number of scheduling variables while maintaining low implementation complexity through affinely scheduled controllers in the case of plants with affine parameter-dependency [16], as is the case in the copolymerization reactor. With both $\mathcal{M}_\phi$ and $\mathcal{M}_\zeta$, the LPV controllers are designed with a fixed Lyapunov function using an $\mathcal{H}_\infty$ loop-shaping approach based on the gain-scheduled LPV synthesis. In order to implement both controllers in reality, the elements of the signal vector $\boldsymbol{\rho}$ (8) should be available to compute $\boldsymbol{\theta}$. Since some of these elements are difficult to measure, the procedure adopted to estimate them is introduced later in this section.

4.1. LPV control synthesis based on $\mathcal{M}_\phi$

The mapped parameter set $\mathbb{P}_\phi$ obtained via (13) allows defining a set of 2^m LTI models, based on which an LPV-$\mathcal{H}_\infty$ controller is synthesized by means of the MATLAB Robust Control toolbox command `hinfgs` [8]. This results in a polytopic LPV controller $\mathcal{K}_\phi$ with the state-space representation

$$\begin{cases} \dot{\boldsymbol{x}}_\mathbf{c}(\boldsymbol{t}) = \boldsymbol{A}_\mathbf{c}(\boldsymbol{\phi}(\boldsymbol{t}))\boldsymbol{x}_\mathbf{c}(\boldsymbol{t}) + \boldsymbol{B}_\mathbf{c}(\boldsymbol{\phi}(\boldsymbol{t}))\boldsymbol{e}(\boldsymbol{t}), \\ \boldsymbol{u}(\boldsymbol{t}) = \boldsymbol{C}_\mathbf{c}(\boldsymbol{\phi}(\boldsymbol{t}))\boldsymbol{x}_\mathbf{c}(\boldsymbol{t}) + \boldsymbol{D}_\mathbf{c}(\boldsymbol{\phi}(\boldsymbol{t}))\boldsymbol{e}(\boldsymbol{t}), \end{cases} \tag{29}$$

where $\boldsymbol{x}_\mathbf{c}$ is the state vector of the controller and the matrix functions $\boldsymbol{A}_\mathbf{c}, \boldsymbol{B}_\mathbf{c}, \boldsymbol{C}_\mathbf{c}$ and $\boldsymbol{D}_\mathbf{c}$ are affine in $\boldsymbol{\phi}(\boldsymbol{t})$; $\mathcal{K}_\phi$ is scheduled with respect to the reduced scheduling

variable $\boldsymbol{\phi(t)}$ according to (29). Note that the controller can still receive the information of T_r via the functions shown in (34) in the Appendix.

The control design objective is to stabilize the closed-loop system in the operating range defined in Table 2 with a fast tracking capability and disturbance rejection taking into consideration the control input constraints as [3]

$$\begin{aligned} 0 \leq & \frac{F_\mathrm{a}}{F_\mathrm{b}} \leq \frac{36}{90}, \\ 0 \leq & F_\mathrm{b} \leq 180 \text{ kg/h}, \\ 0 \leq & \frac{F_\mathrm{c}}{F_\mathrm{b}} \leq \frac{5.4}{90}, \\ 317.754 \leq & T_\mathrm{j} \leq 388.366 \text{ K}. \end{aligned}$$

A standard mixed sensitivity loop-shaping approach is adopted to meet the design objectives. The following weighting filters are selected:

$$\begin{aligned} \boldsymbol{W_\mathbf{S}} &= \mathrm{diag}\left(\frac{5.352\times10^{-2}}{s+7.49\times10^{-3}}, \frac{4.645\times10^{-6}}{s+6.46\times10^{-6}}, \frac{3.043\times10^{-2}}{s+5.18\times10^{-7}} \right), \\ \boldsymbol{W_{\mathbf{KS}}} &= \mathrm{diag}\left(\frac{7.585s+197}{s+2.597\times10^{4}}, \frac{90.77s+9587}{s+1.056\times10^{5}}, \frac{9.862s+11.37}{s+1153} \right). \end{aligned}$$

The sensitivity weighting filter $\boldsymbol{W_\mathbf{S}}$ is responsible for tuning the closed-loop bandwidth and ensuring almost zero steady-state error. The required bandwidth has been inferred from the set of 2^m LTI models of the form (14) after freezing the mapped parameter set $\mathbb{P}_\phi$. On the other hand, the complementary sensitivity weighting filter $\boldsymbol{W_{\mathbf{KS}}}$ has been adjusted to impose an upper bound on the control sensitivity in order to restrict the control effort and reduce the output overshoot. The generalized plant is shown in Fig. 3.

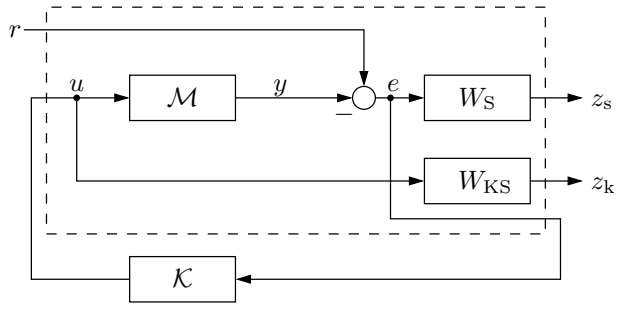

Figure 3: Generalized plant interconnected with the LPV controller.

The complexity of the LPV model via PSM procedure is ideally reduced into one scheduling variable, which allows a minimal design complexity for the deduced LPV controllers and can yield high performance. However, these synthesized controllers may not guarantee the achieved closed-loop stability and performance once they are tested with the full nonlinear model of the copoly-

merization reactor since they are designed based on an approximation of the nonlinear model.

4.2. LPV control synthesis based on $\mathcal{M}_\zeta$

In the following, an LPV-LFT gain-scheduling controller is designed based on $\mathcal{M}_\zeta$, which can provide the same input-output behavior as the full nonlinear model in a prespecified operating regime. The $\mathcal{H}_\infty$ loop-shaping approach based on the gain-scheduling LPV synthesis results of [19] requires the formulation of $\mathcal{M}_\zeta$ in an LFT form as

$$\begin{bmatrix} \boldsymbol{\mathcal{A}}(\boldsymbol{\zeta}) & \boldsymbol{\mathcal{B}}(\boldsymbol{\zeta}) \\ \boldsymbol{\mathcal{C}}(\boldsymbol{\zeta}) & \boldsymbol{\mathcal{D}}(\boldsymbol{\zeta}) \end{bmatrix} = \begin{bmatrix} \boldsymbol{A} & \boldsymbol{B_{\mathbf{u}}} \\ \boldsymbol{C_{\mathbf{y}}} & \boldsymbol{D_{\mathbf{yu}}} \end{bmatrix} + \begin{bmatrix} \boldsymbol{B_\zeta} \\ \boldsymbol{D_{\mathbf{y}\zeta}} \end{bmatrix} \boldsymbol{\Gamma}(\boldsymbol{I} - \boldsymbol{D_{\zeta\zeta}}\boldsymbol{\Gamma})^{-1} \begin{bmatrix} \boldsymbol{C_\zeta} & \boldsymbol{D_{\zeta\mathbf{u}}} \end{bmatrix} \tag{30}$$

where $\boldsymbol{\Gamma} = \mathbf{diag}(\boldsymbol{\zeta_1 I_{\mathbf{r}_1}}, \cdots, \boldsymbol{\zeta_{n_\zeta} I_{\mathbf{r}_{n_\zeta}}})$ is a parameter matrix that includes all the scheduling variables provided that $(\boldsymbol{I} - \boldsymbol{D_{\zeta\zeta}}\boldsymbol{\Gamma})^{-1}$ exists for all $\boldsymbol{\zeta} \in \mathbb{P}_\zeta$, i.e., the well-posedness condition. For parameter-affine LPV models, $\boldsymbol{D_{\zeta\zeta}} = \mathbf{0}$. Moreover, for the derived LPV model of the copolymerization reactor, one has $\boldsymbol{D_{\mathbf{yu}}} = \mathbf{0}$, $\boldsymbol{\Gamma} = \mathbf{diag}(\boldsymbol{\zeta_1, \cdots, \zeta_4}) \in \mathbb{R}^{4\times4}$. Since both the plant and the controller correspond to time-varying systems, the $\mathcal{H}_\infty$ norm is interpreted in terms of the induced $\mathcal{L}_2$-gain.

To meet the control design objectives, the closed-loop system is shaped using weighting filter matrices for the sensitivity $\boldsymbol{W_S}$ and the complementary sensitivity $\boldsymbol{W_{KS}}$ channels, (see Fig. 3) as

$$\boldsymbol{W_S} = \mathrm{diag}\left(\frac{8.326\times10^{-2}}{s+9.019\times10^{-4}}, \frac{1.088\times10^{-1}}{s+1.008\times10^{-3}}, \frac{1.193\times10^{-1}}{s+1.084\times10^{-5}}\right),$$
$$\boldsymbol{W_{KS}} = \mathrm{diag}\left(\frac{1642s+3.885\times10^{4}}{s+2.367\times10^{4}}, \frac{641.7s+6.205\times10^{4}}{s+9.67\times10^{4}}, \frac{1679s+1243}{s+740.5}\right).$$

It is worth noting that these weighting filter matrices are different from the ones obtained in the first approach since they are tuned with different reduced LPV models $\mathcal{M}_\phi$ and $\mathcal{M}_\zeta$. Given $\boldsymbol{W_S}$ and $\boldsymbol{W_{KS}}$, an LFT representation of the generalized plant is obtained as

$$\begin{bmatrix} \tilde{\boldsymbol{\mathcal{A}}}(\boldsymbol{\zeta}) & \tilde{\boldsymbol{\mathcal{B}}}_{\mathbf{p}}(\boldsymbol{\zeta}) & \tilde{\boldsymbol{\mathcal{B}}}(\boldsymbol{\zeta}) \\ \tilde{\boldsymbol{\mathcal{C}}}_{\mathbf{p}}(\boldsymbol{\zeta}) & \tilde{\boldsymbol{\mathcal{D}}}_{\mathbf{pp}}(\boldsymbol{\zeta}) & \tilde{\boldsymbol{\mathcal{D}}}_{\mathbf{pu}}(\boldsymbol{\zeta}) \\ \tilde{\boldsymbol{\mathcal{C}}}(\boldsymbol{\zeta}) & \tilde{\boldsymbol{\mathcal{D}}}_{\mathbf{yp}}(\boldsymbol{\zeta} & \tilde{\boldsymbol{\mathcal{D}}}(\boldsymbol{\zeta}) \end{bmatrix} = \begin{bmatrix} \tilde{\boldsymbol{A}} & \tilde{\boldsymbol{B}}_{\mathbf{p}} & \tilde{\boldsymbol{B}}_{\mathbf{u}} \\ \tilde{\boldsymbol{C}}_{\mathbf{p}} & \tilde{\boldsymbol{D}}_{\mathbf{pp}} & \tilde{\boldsymbol{D}}_{\mathbf{pu}} \\ \tilde{\boldsymbol{C}}_{\mathbf{y}} & \tilde{\boldsymbol{D}}_{\mathbf{yp}} & \tilde{\boldsymbol{D}}_{\mathbf{yu}} \end{bmatrix} + \begin{bmatrix} \tilde{\boldsymbol{B}}_{\boldsymbol{\zeta}} \\ \tilde{\boldsymbol{D}}_{\mathbf{p}\boldsymbol{\zeta}} \\ \tilde{\boldsymbol{D}}_{\mathbf{y}\boldsymbol{\zeta}} \end{bmatrix} \boldsymbol{\Gamma} \begin{bmatrix} \tilde{\boldsymbol{C}}_{\boldsymbol{\zeta}} & \tilde{\boldsymbol{D}}_{\boldsymbol{\zeta}\mathbf{p}} & \tilde{\boldsymbol{D}}_{\boldsymbol{\zeta}\mathbf{u}} \end{bmatrix}.$$

Then, a *linear matrix inequality* (LMI) condition for the existence of a gain-scheduled $\mathcal{H}_\infty$ controller in an LFT form [19] based on the so-called multipliers is employed. In order to synthesize an affinely gain-scheduled controller such that the scheduling block $\boldsymbol{\Gamma}$ of the plant is *copied* to the controller, the multipliers are chosen according to [28].

The parameter-dependent state-space model matrices of the affinely scheduled controller $\mathcal{K}_\zeta$ are then computed by

$$\begin{bmatrix} \boldsymbol{\mathcal{A}}_{\mathbf{c}}(\boldsymbol{\zeta}) & \boldsymbol{\mathcal{B}}_{\mathbf{c}}(\boldsymbol{\zeta}) \\ \boldsymbol{\mathcal{C}}_{\mathbf{c}}(\boldsymbol{\zeta}) & \boldsymbol{\mathcal{D}}_{\mathbf{K}}(\boldsymbol{\zeta}) \end{bmatrix} = \begin{bmatrix} \boldsymbol{A}^{\mathbf{c}} & \boldsymbol{B}^{\mathbf{c}}_{\mathbf{u}} \\ \boldsymbol{C}^{\mathbf{K}}_{\mathbf{y}} & \boldsymbol{D}^{\mathbf{c}}_{\mathbf{yu}} \end{bmatrix} + \begin{bmatrix} \boldsymbol{B}^{\mathbf{c}}_{\boldsymbol{\zeta}} \\ \boldsymbol{D}^{\mathbf{c}}_{\mathbf{y}\boldsymbol{\zeta}} \end{bmatrix} \boldsymbol{\Gamma} \begin{bmatrix} \boldsymbol{C}^{\mathbf{c}}_{\boldsymbol{\zeta}} & \boldsymbol{D}^{\mathbf{c}}_{\boldsymbol{\zeta}\mathbf{u}} \end{bmatrix}, \tag{31}$$

which is a 10^{th} order 3×3 LPV controller for the problem under study. In terms of the control implementation, the LPV controller (31) requires relatively low online computation as it only needs to update the controller state-space matrices at each time instant given the value of the $\boldsymbol{\Gamma}$ block; see [16] for more details about the implementation complexity of LPV controllers.

It is important to point out that the implementation of LPV controllers $\mathcal{K}_\phi$ and $\mathcal{K}_\zeta$ based on the designed LPV models requires the possibility of measuring or estimating $\boldsymbol{\rho}$ chosen in (8) at every time instant. Therefore, the next section is dedicated to design an extended Kalman filter in order to estimate $\boldsymbol{\rho}$.

4.3. An extended Kalman filter to estimate $\boldsymbol{\rho}$

The availability of the vector $\boldsymbol{\rho}$ is required at each sampling time instant in order to compute the scheduling variable $\boldsymbol{\theta}$ and consequently $\boldsymbol{\phi}$ or $\boldsymbol{\zeta}$ for the controller $\mathcal{K}_\phi$ or $\mathcal{K}_\zeta$. In the copolymerization reactor model, the flow rate and composition of the feed F_k ($k = \mathrm{a}, \mathrm{b}, \mathrm{i}, \mathrm{s}, \mathrm{t}, \mathrm{z}$) are measured along with the reactor temperature T_r [4, 26, 29]. On other hand, the molecular weight is measured online using a capillary viscometer as described in [4], and the copolymer product composition is measured using nuclear magnetic resonance (NMR) spectroscopy. As discussed in [4], the on-line measurements of polymer architecture such as composition and molecular weight may be simply unavailable. Moreover, the choice of sampling frequency depends on the requirements for good quality control and the need to minimize analytical costs. Usually, when the reactor residence time is much shorter than the sampling frequency, integral control is appropriate. In other cases, the sampling time introduced by the periodic analysis of polymer concentration, polymer composition, and molecular weight may not be long enough so the incorporation of online state estimators of polymer properties is necessary [4].

As a result of the above analysis, the elements of $\boldsymbol{\rho}$ that must be estimated are $\boldsymbol{\rho}^{\mathbf{est}} = [C_\mathrm{a},\ C_\mathrm{b},\ C_\mathrm{i},\ C_\mathrm{s},\ C_\mathrm{t},\ C_\mathrm{z},\ \lambda_\mathrm{a},\ \lambda_\mathrm{b},\ \psi_1]$. Consequently, the estimation of the state vector for the copolymerization reactor model (1) is required. In [26], the same copolymerization reactor model as (1) was used to develop an extended discrete-time Kalman filter for state estimation. For more realistic study, an additive disturbance is added to the measurements. In this paper, a continuous-time extended Kalman filter is applied for the nonlinear model of the copolymerization reactor (1) which can be written as

$$\begin{aligned} \dot{\boldsymbol{x}}(\boldsymbol{t}) &= \boldsymbol{f}\big(\boldsymbol{x}(\boldsymbol{t}), \boldsymbol{u}(\boldsymbol{t})\big) + \boldsymbol{w}(\boldsymbol{t}), \\ \boldsymbol{y}(\boldsymbol{t}) &= \boldsymbol{h}\big(\boldsymbol{x}(\boldsymbol{t})\big) + \boldsymbol{v}(\boldsymbol{t}), \end{aligned} \tag{32}$$

where $\boldsymbol{f}\big(\boldsymbol{x(t)}, \boldsymbol{u(t)}\big)$ and $\boldsymbol{h}\big(\boldsymbol{x(t)}\big)$ are nonlinear functions and $\boldsymbol{w(t)}$ and $\boldsymbol{v(t)}$ are the process and observation noises assumed to be zero mean Gaussian noises with covariance $\boldsymbol{R(t)}$ and $\boldsymbol{Q(t)}$, respectively. The extended Kalman filter is implemented as follows:
Initialization step:

$$\hat{\boldsymbol{x}}(\boldsymbol{t_0}) = \mathrm{E}\big[\boldsymbol{x(t_0)}\big],\ \boldsymbol{P(t_0)} = \mathbf{Var}\big[\boldsymbol{x(t_0)}\big]$$

Prediction and update steps:

$$\begin{aligned}
\dot{\hat{\boldsymbol{x}}}(\boldsymbol{t}) &= \boldsymbol{f}\big(\hat{\boldsymbol{x}}(\boldsymbol{t}), \boldsymbol{u(t)}\big) + \boldsymbol{K(t)}\Big(\boldsymbol{y(t)} - \boldsymbol{h}\big(\hat{\boldsymbol{x}}(\boldsymbol{t})\big)\Big),\\
\dot{\boldsymbol{P}}(\boldsymbol{t}) &= \boldsymbol{F(t)P(t)} + \boldsymbol{P(t)F(t)}^{\top} - \boldsymbol{K(t)H(t)P(t)} + \boldsymbol{R(t)},\\
\boldsymbol{K(t)} &= \boldsymbol{P(t)H(t)}^{\top}\boldsymbol{Q(t)}^{-1},\\
\boldsymbol{F(t)} &= \left.\frac{\partial \boldsymbol{f}}{\partial \boldsymbol{x}}\right|_{\hat{\boldsymbol{x}}(\boldsymbol{t}), \boldsymbol{u(t)}},\\
\boldsymbol{H(t)} &= \left.\frac{\partial \boldsymbol{h}}{\partial \boldsymbol{x}}\right|_{\hat{\boldsymbol{x}}(\boldsymbol{t})},
\end{aligned} \tag{33}$$

where $\boldsymbol{P(t)}$ is the covariance estimate and $\boldsymbol{K(t)}$ is the Kalman filter gain.

5. Implementation of the EKF-based LPV controllers

The control design objectives that are considered in this paper are the same as those in [3]. It is basically required to examine the effect of the transition from OP1 to OP2 as shown in Table 2, for each of the four output variables. The designed controllers have been simulated with the nonlinear model of the copolymerization reactor (1). For the output T_{r}, a tuned PI controller is considered based on the design procedure discussed in [6]; this is justified as the change of T_{r} from OP1 to OP2 is very small. In order to compute the state-space matrices of the controllers via (29) and (31) at each sampling instant, the estimation of $\boldsymbol{\rho}^{\mathbf{est}}$, which is the unmeasurable part of $\boldsymbol{\rho}$, is obtained by means of the extended Kalman filter (33). The measurement noises added to the output signals are equal to 3% of the operating point except for T_{r}, for which the added noise is 1% [30] (see Fig. 4). A comparative analysis of the closed-loop performance is done between the LPV controllers synthesized for both modeling approaches and the model predictive controller (MPC) developed in [3].

5.1. Implementation with the LPV controller $\mathcal{K}_\phi$

The state vector is estimated by the extended Kalman filter for the nonlinear model of the copolymerization reactor (1). The highly accurate estimation of the most important state variables is shown in Figure 5. The resulting input flow rates and the estimated outputs during the transition from OP1 to OP2 with the controller $\mathcal{K}_\phi$ are shown in Figures 6a and 6b. The real outputs (without noise) coincide with the estimated ones as seen in Figure 6b. A fast

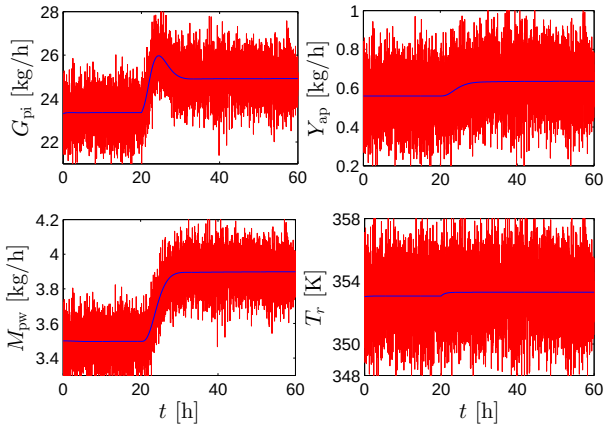

Figure 4: Real (blue line) and noisy (red line) output measurements.

convergence of the temperature $T_{\rm r}$ is achieved. The production rate $G_{\rm pi}$, the polymer composition $Y_{\rm ap}$ and the molecular weight $M_{\rm pw}$ take almost 9 hours to reach their steady states. This result emphasizes the importance of PCA in reducing the model complexity for developing a controller, as well as in providing enhanced closed-loop performance.

It is important to note that the target of the controller K_ϕ is to get Y_{ap} to reach 0.64 as shown in Figure 6b. It reached 0.636 that is equivalent to 0.6% of error, which is acceptable. The reason is that the controller K_ϕ designed based on a mixed sensitivity loop-shaping approach cannot provide a pure integral action that does achieve zero steady state error. A steady-state error up to $\pm 1\%$ could be considered to be reasonable. Hence, such an objective in terms of the shaping filters was used during the control synthesis.

5.2. Implementation with the LPV controller $\mathcal{K}_\zeta$

The implementation of the LPV controller $\mathcal{K}_\zeta$ on the full nonlinear model of the plant is shown in Figures 6a and 6b, which illustrate the input and the closed-loop output responses, respectively, during the transition from OP1 to OP2. As observed in [3], the production rate $G_{\rm pi}$ and the temperature $T_{\rm r}$ show faster response in comparison with the polymer composition $Y_{\rm ap}$ and the molecular weight $M_{\rm pw}$; however, all outputs require less than 10 hours to reach the steady-state values without violating the input constraints.

Next, the results of our comparative study of the performance of the controllers synthesized for both approaches and the MPC controller proposed in [3] are reported. As shown in Table 4, $\mathcal{K}_\phi$ provides a better performance than the controller $\mathcal{K}_\zeta$ and the MPC controller. The convergence time of $\mathcal{K}_\phi$ is the lowest and, unlike the other two methods, the outputs $Y_{\rm ap}$, $M_{\rm pw}$ and $T_{\rm r}$ in Fig. 6b do

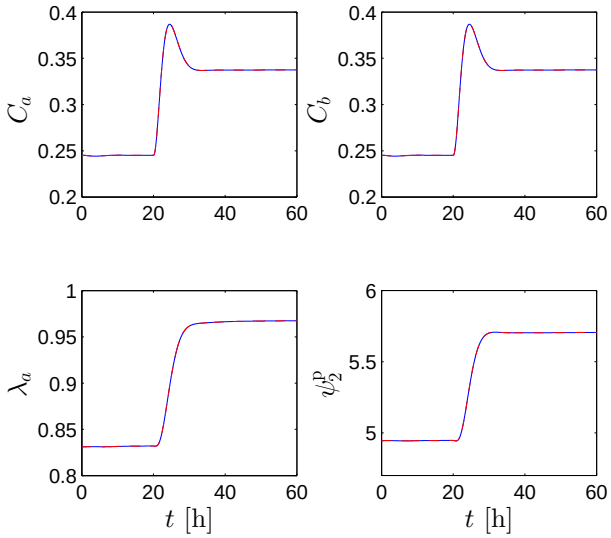

Figure 5: Estimated state variables during the transition from OP1 to OP2: actual (blue line) and estimated (red dashed line).

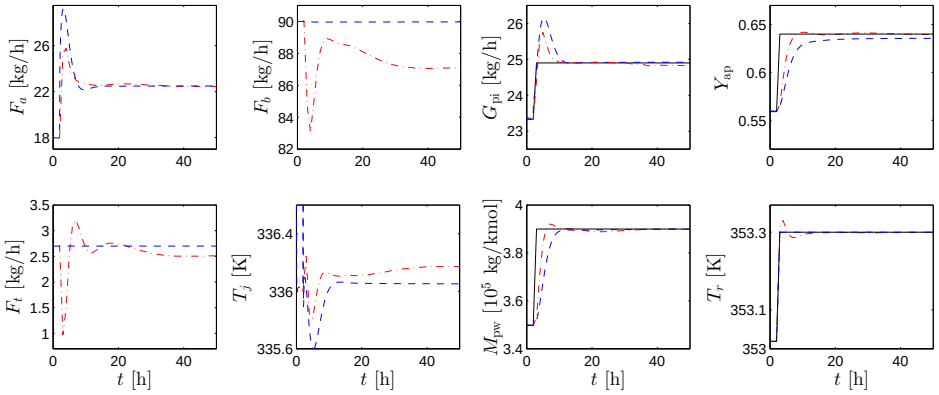

(a) Manipulated variables (b) Closed-loop response

Figure 6: (a) Manipulated variables, and (b) closed-loop response: reference (solid black line) with $\mathcal{K}_\phi$ (blue dashed line) and $\mathcal{K}_\zeta$ (red dash-dotted line) during the transition from OP1 to OP2.

not exhibit any overshoot. On the other hand, the input flow rates of $\mathcal{K}_\zeta$ and those of $\mathcal{K}_\phi$ in Figure 6a do not saturate and the overshoots are less than those shown in [3]. The improvement brought by $\mathcal{K}_\phi$ in the output settling time and the input quality has a significant impact on the industrial process of polymer

production.

Table 4: Closed-loop performance of the LPV controllers and MPC.

		$\mathcal{K}_\phi$	$\mathcal{K}_\zeta$	MPC
Convergence time (h)		9	10	15
Input overshoots (%)	F_a	17	15.5	50
	F_b	0.5	4	11
	F_t	≈ 0	≈ 0	18
	T_j	≈ 0	60	0.5
Output overshoots(%)	G_pi	4.4	3.4	6.4
	Y_ap	0	≈ 0	0
	M_pw	0	0.7	0
	T_r	0	≈ 0	≈ 0

Finally, the effect of an unmeasured disturbance is examined while taking into consideration the presence of an inhibitor flow in the fresh feed during the transition from OP1 to OP2, i.e., $F_\mathrm{z} \neq 0$. The capability of the LPV controllers is demonstrated for an inhibitor disturbance of 4 parts per thousand (mole basis) during the period (1.5-3.0 h) as in [3]. Unlike the MPC controller developed in [3], $\mathcal{K}_\phi$ and $\mathcal{K}_\zeta$ (Figure 7a) prevent the saturation of the input flow rates. Also, these controllers reject the disturbance effect without showing aggressive response as illustrated in Figure 7b. Furthermore, with $\mathcal{K}_\phi$, no oscillations are observed and the convergence interval (around 10 hours) is slower than the case without disturbance; however, it remains faster than the response of $\mathcal{K}_\zeta$ that takes 30 hours to reach the desired values, as well as the response of MPC controller in [3] which takes more than 15 hours to converge. In addition, in [3], the convergence time of the polymer composition Y_ap is longer than 30 hours.

It is worth to mention that the synthesis complexity of $\mathcal{K}_\phi$ is much lower than that of $\mathcal{K}_\zeta$ as the scheduling dimension of the former is one, whereas it is 4 with the latter. This reduces the complexity of $\mathcal{K}_\phi$ and demonstrates the improvement of its achieved performance. On the other hand, $\mathcal{K}_\phi$ cannot guarantee closed-loop stability (theoretically) when it is implemented on the nonlinear process as it is based on the approximate model $\mathcal{M}_\phi$. However, given the exact state estimation, a theoretical stability can be guaranteed with $\mathcal{K}_\zeta$ for all $\boldsymbol{\zeta} \in \mathbb{P}_\zeta$ as it is designed based on the exact model $\mathcal{M}_\zeta$. A trade-off is illustrated between the design complexity and performance of the LPV controller on one hand, and the stability guarantee of the closed-loop with the nonlinear process on other hand.

6. Conclusions

In this paper, two different approaches are proposed to reduce the large number of scheduling variables in the LPV model of the copolymerization reactor. In the first approach, the parameter set mapping based on principal component

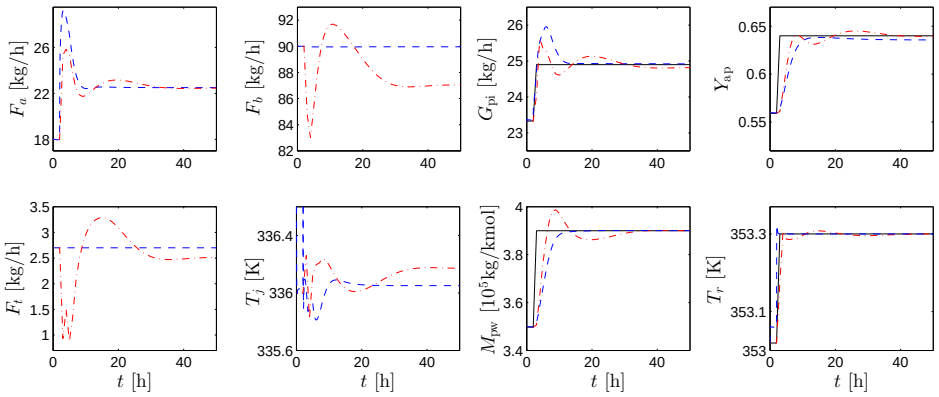

(a) Manipulated variables (b) Closed-loop response

Figure 7: (a) Manipulated variables, and (b) closed-loop response: reference (solid black line) with $\mathcal{K}_\phi$ (blue dashed line) and $\mathcal{K}_\zeta$ (red dash-dotted line) during the transition from OP1 to OP2 in the presence of a disturbance.

analysis has been employed to reduce the number of scheduling variables resulting from LPV modeling. In the second approach, a low complexity LPV model has been derived by reformulating the representation of the nonlinear model. Based on the developed LPV models, an LPV controller has been designed for the LPV model obtained with each of the approaches. An extended Kalman filter is designed to estimate the unmeasurable state variables. The performance of the extended Kalman filter-based controllers applied to the original nonlinear model has been compared for a transition between two operating points of the copolymerization reactor. The LPV controller $\mathcal{K}_\phi$, based on one scheduling dimension LPV model, has shown a better disturbance rejection without either output oscillation or input saturation. This enhancement in the closed-loop performance is due to the low conservatism of the design by the PSM approach. However, the inability to guarantee the closed-loop stability with the nonlinear reactor model remains the main drawback of the PSM procedure. The stability is, however, guaranteed with the LPV controller $\mathcal{K}_\zeta$ which is designed based on state truncated model, but its design is more complicated with four scheduling variables. A trade-off is illustrated by the low complexity and good performance on one hand, and the stability guarantee of the closed-loop system with the nonlinear model of the reactor on other hand.

7. Appendix

The scheduling variables $\theta_1, \ldots, \theta_{15}$ in the LPV representation of the copolymerization reactor in (3) are defined as

$$
\begin{aligned}
\theta_1 &= \frac{1}{\theta_{\mathrm{r}}} = f_1(F_{\mathrm{a}}\ F_{\mathrm{b}}\ F_{\mathrm{i}}\ F_{\mathrm{s}}\ F_{\mathrm{t}}\ F_{\mathrm{z}}),\\
\theta_{2-7} &= \frac{R_k}{C_k}\ (k = a, b, i, s, t, z) = f_{2-7}(C_{\mathrm{a}}, C_{\mathrm{b}}, C_{\mathrm{i}}, C_{\mathrm{z}}, T_{\mathrm{r}}),\\
\theta_8 &= \frac{1}{2}\left(k_{\mathrm{caa}}(\psi_0^{\mathrm{a}\cdot})^2 + k_{\mathrm{cab}}\psi_0^{\mathrm{a}\cdot}\psi_0^{\mathrm{b}\cdot} + L_1\psi_0^{\mathrm{a}\cdot}\right)/C_{\mathrm{a}} = f_8(C_{\mathrm{a}}, C_{\mathrm{b}}, C_{\mathrm{i}}, C_{\mathrm{s}}, C_{\mathrm{t}}, C_{\mathrm{z}}, T_{\mathrm{r}}),\\
\theta_9 &= \frac{1}{2}\left(k_{\mathrm{cbb}}(\psi_0^{\mathrm{b}\cdot})^2 + L_2\psi_0^{\mathrm{b}\cdot}\right)/C_{\mathrm{b}} = f_9(C_{\mathrm{a}}, C_{\mathrm{b}}, C_{\mathrm{i}}, C_{\mathrm{s}}, C_{\mathrm{t}}, C_{\mathrm{z}}, T_{\mathrm{r}}),\\
\theta_{10} &= \left(k_{\mathrm{caa}}\psi_0^{\mathrm{a}\cdot}\psi_1^{\mathrm{a}\cdot} + k_{\mathrm{cab}}(\psi_0^{\mathrm{b}\cdot}\psi_1^{\mathrm{a}\cdot}) + L_1\psi_1^{\mathrm{a}\cdot}\right)/C_{\mathrm{a}} = f_{10}(C_{\mathrm{a}}, C_{\mathrm{b}}, C_{\mathrm{i}}, C_{\mathrm{s}}, C_{\mathrm{t}}, C_{\mathrm{z}}, T_{\mathrm{r}}),\\
\theta_{11} &= \left(k_{\mathrm{cab}}(\psi_0^{\mathrm{a}\cdot}\psi_1^{\mathrm{b}\cdot}) + k_{\mathrm{cbb}}\psi_0^{\mathrm{b}\cdot}\psi_1^{\mathrm{b}\cdot} + L_2\psi_1^{\mathrm{b}\cdot}\right)/C_{\mathrm{b}} = f_{11}(C_{\mathrm{a}}, C_{\mathrm{b}}, C_{\mathrm{i}}, C_{\mathrm{s}}, C_{\mathrm{t}}, C_{\mathrm{z}}, T_{\mathrm{r}}),\\
\theta_{12} &= \left(k_{\mathrm{caa}}\left((\psi_1^{\mathrm{a}\cdot})^2 + \psi_0^{\mathrm{a}\cdot}\psi_2^{\mathrm{a}\cdot}\right) + k_{\mathrm{cab}}(2\psi_1^{\mathrm{a}\cdot}\psi_1^{\mathrm{b}\cdot} + \psi_2^{\mathrm{b}\cdot}\psi_0^{\mathrm{a}\cdot}) + L_1\psi_2^{\mathrm{a}\cdot}\right)/C_{\mathrm{a}}\\
&= f_{12}(C_{\mathrm{a}}, C_{\mathrm{b}}, C_{\mathrm{i}}, C_{\mathrm{s}}, C_{\mathrm{t}}, C_{\mathrm{z}}, T_{\mathrm{r}}),\\
\theta_{13} &= \left(k_{\mathrm{cab}}(\psi_2^{\mathrm{a}\cdot}\psi_0^{\mathrm{b}\cdot}) + k_{\mathrm{cbb}}\left((\psi_1^{\mathrm{b}\cdot})^2 + \psi_0^{\mathrm{b}\cdot}\psi_2^{\mathrm{b}\cdot}\right) + L_2\psi_2^{\mathrm{b}\cdot}\right)/C_{\mathrm{b}}\\
&= f_{13}(C_{\mathrm{a}}, C_{\mathrm{b}}, C_{\mathrm{i}}, C_{\mathrm{s}}, C_{\mathrm{t}}, C_{\mathrm{z}}, T_{\mathrm{r}}),\\
\theta_{14} &= \frac{1}{\psi_1^{\mathrm{p}}} = f_{14}(\psi_1^{\mathrm{p}}),\\
\theta_{15} &= \frac{1}{\lambda_{\mathrm{a}} + \lambda_{\mathrm{b}}} = f_{15}(\lambda_{\mathrm{a}}, \lambda_{\mathrm{b}}).
\end{aligned}
\tag{34}
$$

An example of representing the dynamics of the first state $\left(\frac{\mathrm{d}C_{\mathrm{a}}}{\mathrm{d}t}\right)$ in the LPV form is shown as follows:

$$
\begin{aligned}
\tfrac{\mathrm{d}C_{\mathrm{a}}}{\mathrm{d}t} &= \tfrac{C_{\mathrm{af}}}{\theta_{\mathrm{r}}} - \tfrac{1}{\theta_{\mathrm{r}}}C_{\mathrm{a}} - \tfrac{R_{\mathrm{a}}}{C_{\mathrm{a}}}C_{\mathrm{a}}\\
&= \tfrac{1}{M_{\mathrm{a}}V_{\mathrm{r}}}F_{\mathrm{a}} - \underbrace{\frac{\sum_k F_k}{\rho_{\mathrm{r}}V_{\mathrm{r}}}}_{\theta_1}C_{\mathrm{a}}\\
&\quad - \underbrace{\left(\frac{(k_{\mathrm{paa}} + k_{\mathrm{xaa}})\, g_2(C_{\mathrm{a}}, C_{\mathrm{b}}, C_{\mathrm{i}}, C_{\mathrm{z}})}{g_1(C_{\mathrm{a}}, C_{\mathrm{b}})} + \frac{C_{\mathrm{b}}(k_{\mathrm{pab}} + k_{\mathrm{xab}})\, g_2(C_{\mathrm{a}}, C_{\mathrm{b}}, C_{\mathrm{i}}, C_{\mathrm{z}})}{C_{\mathrm{a}}\, g_1(C_{\mathrm{a}}, C_{\mathrm{b}})}\right)}_{\theta_2}C_{\mathrm{a}}\\
&= \tfrac{1}{M_{\mathrm{a}}V_{\mathrm{r}}}F_{\mathrm{a}} - (\theta_1 + \theta_2)C_{\mathrm{a}}
\end{aligned}
\tag{35}
$$

where the kinetic parameters k are function of T_{r} (see [6]) and $g_1(C_{\mathrm{a}}, C_{\mathrm{b}})$ and $g_2(C_{\mathrm{a}}, C_{\mathrm{b}}, C_{\mathrm{i}}, C_{\mathrm{z}})$ are nonlinear functions.

References

[1] M. Embirucu, E. Lima, J. Pinto, A survey of advanced control of polymerization reactors, Polymer Engineering and Science 36 (4) (1996) 433–447.

[2] M. Soroush, C. Kravaris, Multivariable nonlinear control of a continuous polymerization reactor: an experimental study, American Institute of Chemical Engineers Journal (AIChE) 39 (12) (1993) 1920–1937.

[3] L. Özkan, M. V. Kothare, C. Georgakis, Control of a solution copolymerization reactor using multi-model predictive control, Chemical Engineering Science 58 (7) (2003) 1207–1221.

[4] J. R. Richards, J. P. Congalidis, Measurement and control of polymerization reactors, Computers & chemical engineering 30 (10) (2006) 1447–1463.

[5] J. P. Congalidis, J. R. Richards, Process control of polymerization reactors: An industrial perspective, Polymer Reaction Engineering 6 (2) (1998) 71–111.

[6] J. Congalidis, J. Richarards, W. H. Ray, Feedforward and feedback control of a solution copolymerization reactor, American Institute of Chemical Engineers (A.I.Ch.E.) Journal 35 (6) (1989) 891–907.

[7] B. Maner, F. Doyle, Polymerization reactor control using autoregressive-plus Volterra-based MPC, American Institute of Chemical Engineers (AIChE) Journal 43 (7) (1997) 1763–1784.

[8] P. Apkarian, P. Gahinet, G. Becker, Self-scheduled H_∞ control of linear parameter-varying systems: a design example, Automatica 31 (9) (1995) 1251–1261.

[9] W. J. Rugh, J. S. Shamma, Research on gain scheduling, Automatica 36 (2000) 1401–1425.

[10] R. Tóth, Modeling and Identification of Linear Parameter-Varying Systems, Springer–Verlag, Berlin, Heidelberg.

[11] J. Mohammadpour, C. Scherer, Control of Linear Parameter Varying Systems with Applications, Springer-Verlag, New York Dordrecht Heidelberg London, 2012.

[12] R. Tóth, M. Van de Wal, P. Heuberger, P. Van den Hof, LPV identification of high performance positioning devices, in: Proc. of the American Control Conference, San Francisco, CA, USA, 2011, pp. 151–158.

[13] H. S. Abbas, A. Ali, S. M. Hashemi, H. Werner, LPV state-feedback control of a control moment gyroscope, Control Engineering Practice 24 (3) (2014) 129–137.

[14] A. Bachnas, R. Tóth, J. Ludlage, A. Mesbah, A review on data-driven linear parameter-varying modeling approaches: A high-purity distillation column case study, Journal of Process Control 24 (4) (2014) 272–285.

[15] A. Kwiatkowski, H. Werner, Parameter reduction for LPV systems via principle components analysis, in: Proc. 16$^{\text{th}}$ IFAC World Congress, Prague, Czech Republic, 2005.

[16] C. Hoffmann, H. Werner, Complexity of implementation and synthesis in linear parameter-varying control, Proc. of the 19$^{\text{th}}$ IFAC World Congress (2014) 11749–11760.

[17] T. Azuma, R. Watanabe, K. Uchida, M. Fujita, A new LMI approach to analysis of linear systems depending on scheduling parameters in polynomial forms, Automatisierungstechnik Methoden und Anwendungen der Steuerungs-, Regelungs-und Informationstechnik 48 (4) (2000) 119–204.

[18] A. Kwiatkowski, LPV Modeling and Application of LPV Controllers to SI Engines, Ph.D. dissertation, Hamburg University of Technology, Germany, 2008.

[19] C. Scherer, LPV control and full block multipliers, Automatica 27 (3) (2001) 325–485.

[20] H. W. Sorenson, Kalman filtering: theory and application, IEEE Press, 1985.

[21] A. D. Schmidt, W. H. Ray, The dynamic behavior of continuous polymerization reactors-i isothermal solution polymerization in a cstr, Chemical Engineering Science 36 (12) (1981) 1401–1410.

[22] A. D. Schmidt, W. H. Ray, The dynamic behavior of continuous polymerization reactors-ii isothermal solution polymerization in a cstr, Chemical Engineering Science 36 (12) (1981) 1897–1914.

[23] A. D. Schmidt, A. B. Clinch, W. H. Ray, The dynamic behavior of continuous polymerization reactors-iii: An experimental study of multiple steady states in solution polymerization, Chemical Engineering Science 39 (3) (1984) 419–432.

[24] F. Teymour, W. H. Ray, The dynamic behavior of continuous polymerization reactors-iv: Dynamic stability and bifurcation analysis of an experimental reactor, Chemical Engineering Science 44 (9) (1989) 1967–1982.

[25] F. Teymour, W. H. Ray, The dynamic behavior of continuous polymerization reactors-v: Experimental investigation of limit-cycle behavior for vinyl acetate polymerization, Chemical Engineering Science 47 (15/16) (1992) 4121–4132.

[26] R. Bindlish, J. B. Rawlings, Target linearization and model predictive control of polymerization processes, AIChE journal 49 (11) (2003) 2885–2899.

[27] S. M. Hashemi, H. Abbas, H. Werner, Low-complexity linear parameter-varying modeling and control of a robotic manipulator, Control Engineering Practice 20 (3) (2012) 248–257.

[28] C. Hoffmann, S. Hashemi, H. Abbas, H. Werner, Synthesis of LPV controllers with low implementation complexity based on a reduced parameter set, Control Systems Technology, IEEE Transactions on 22 (6) (2014) 2393–2398.

[29] W. J. Yoon, Y. S. Kim, I. S. Kim, K. Y. Choi, Recent advances in polymer reaction engineering: modeling and control of polymer properties, Korean Journal of Chemical Engineering 21 (1) (2004) 147–167.

[30] A. Sirohi, K. Y. Choi, On-line parameter estimation in a continuous polymerization process, Industrial & engineering chemistry research 35 (4) (1996) 1332–1343.